Hindawi
Journal of Applied Mathematics
Volume 2022, Article ID 6988197, 12 pages
https://doi.org/10.1155/2022/6988197

Research Article

Modelling and Stability Analysis of Cotton Leaf Curl Virus (CLCuV) Transmission Dynamics in Cotton Plant

Abayneh Kebede Fantaye

Department of Mathematics, Debre Tabor University, Ethiopia

Correspondence should be addressed to Abayneh Kebede Fantaye; abayk400@gmail.com

Received 25 April 2022; Revised 22 July 2022; Accepted 28 July 2022; Published 16 August 2022

Academic Editor: Qiankun Song

In this paper, the transmission dynamics of cotton leaf curl virus (CLCuV) disease in cotton plants was proposed and investigated qualitatively using the stability theory of a nonlinear ordinary differential equations. Cotton and vector populations were both taken into account in the models. Cotton population was categorized as susceptible (A) and infected (B). The vector population was also categorized as susceptible (C) and infected (D). We established that all model solutions are positive and bounded by relevant initial conditions. The existence of unique CLCuV free and endemic equilibrium points, as well as the basic reproduction number, which is computed using the next generation matrix approach, are investigated. The conditions for the local and global asymptotic stability of these equilibrium points are then established. When the basic reproduction number is less than one, the system has locally and globally asymptotically stable CLCuV free equilibrium point, but when the basic reproduction number is more than one, the system has locally and globally asymptotically stable endemic equilibrium point. The numerical simulation findings show that lowering the infection rate of cotton vectors has a significant impact on controlling cotton leaf curl virus (CLCuV) in the time frame given.

1. Introduction

Cotton (Gossypium spp.) is the most significant fiber, oil, and protein crop on the planet (Monga and Sain [1]). Cotton is well-known for its versatility, performance, attractiveness, natural comfort, and, most importantly, its many applications, which include astronaut in-flight space suits, towels, tarpaulins, tents, sheets, and all types of clothing (Vanitha et al. [2]). It is referred to as "white gold, " and it is one of the most important crops in developing countries, as well as a raw material for the local textile and oil industries (Sain et al. [3]). Cotton is significant since it is not only the world's most important fiber crop, but also the world's second-largest oilseed crop (Zhang et al. [4]).

The majority of Ethiopian cotton is exported to Africa, Asia, and Europe, with Asia accounting for 67% of total exports. Ethiopian cotton has now been priced by the Textile Industry Development Institute (Zeleke et al. [5]). The leaf is the most susceptible to diseases, which cause plant damage and death (Kumar et al. [6]). Cotton leaf curl virus (CLCuV) disease is caused by a group of viruses in the genus Begomovirus, which is spread by whiteflies and poses a serious threat to the cotton crop (Farooq et al. [7]). It can be found in Africa, Pakistan, and Northwestern India (Sattar et al. [8]).

Cotton symptoms often appear 2-3 weeks after B. tabaci inoculation (and are characterized by a deep downward cupping of the youngest leaves). Cotton plant infected with CLCuV exhibits thickening and yellowing veins, upward and downward curling, enations on the underside of the leaves, and stunting. CLCuV control relies on insecticide treatments against the insect vector Bemisia tabaci (Briddon) [9].

The mathematical modeling of crop disease in plant pathology is presently a rapidly emerging topic. Fouda et al. [10] constructed a mathematical model of bleached cotton plain single jersey knitted fabrics that may be used to anticipate fabric attributes and define fabric geometrical relationships before manufacturing. Furthermore, the fabric measuring method measures the real yarn diameter and estimates the fabric thickness as a result. According to the

findings, the thickness of a simple single jersey is related to three times the yarn diameter.

Levins et al. [11] devised a model that describes the differential equations of interactions between prey and predator, crop and pest, and migration effect. The models were used to find answers to environmental questions.

Hernández-Bautista et al. [12] proposed a mathematical model that portrays cotton dyeing in cones on three scales: micro, meso, and macro. To simulate cotton dyeing, the mass and momentum conservation equations were applied; Banks et al. [13] provided a mathematical model and statistical models, including ANOVA-based model comparison tests and residual plot analysis, that they used to make the best selections. They also investigate the statistical assumptions that are frequently made inadvertently during the parameter estimation process, as well as the effects of making erroneous assumptions.

Mamatov et al. [14] introduced a single parabolic-type boundary value problem for calculating the temperature field of raw cotton and air components in drum dryers. The proposed model and numerical technique are shown to accurately explain the raw cotton drying process. Dome et al. [15] developed a mathematical model for calculating input demand in relation to cotton production costs. They also assert that cotton farmers are very vulnerable to swings in input prices, which determine whether they generate profitable or loss-making output when compared to total costs per hectare.

Monomolecular, Logistic, Gompertz, Richards, Quadratic, and Reciprocal growth models were provided by Sundar Rajan and Palanivel [16] for India Cotton area, output, and productivity statistics from 1980 to 2013. The chosen model had the highest R2, lower residual sum of squares, and mean square error of the six models considered.

Aboukarima et al. [17] created a multiple regression model to forecast the leaf area of a cotton crop for agricultural research purposes. The developed model could be a viable and quick alternative, especially in areas where modern technology or other tools for measuring leaf area are not available.

Su et al. [18] studied leaf area index (LAI) models and the relationships between LAI, dry matter, and yield for cotton cultivated under three soil conditioners in Korla, Xinjiang, China, with the goal of improving water use efficiency and finding optimal soil conditioner application rates. Khan et al. [19] investigated the association between the occurrence of cotton leaf curl virus (CLCuV), environmental circumstances, and the population of silver leaf whiteflies in Pakistan's agricultural sector. The proposed mathematical relationship can anticipate disease incidence in future months, which can aid agriculturists in disease control in Pakistan's agricultural areas.

Ahmad et al. [20] developed a mathematical model of cotton leaf curl viral infection in Pakistan and its link to meteorological variables. They employ mathematics to connect the intensity of the cotton leaf curl virus (CLCuV) to environmental factors including temperature, rainfall, and humidity, as well as the population of whiteflies in Pakistan's agricultural sector. Humidity and rainfall have been connected to the sickness.

Saeed et al. [21] examined cotton leaf curl virus, fiber quality, and yield components in germplasm imported from the United States. 79 cotton genotypes were evaluated using statistical techniques such as correlation analysis, clustering, and principal components. Cotton leaf curl virus demonstrated a substantial negative association with plant height, monopodial and sympodial branches, and a significant positive relationship with fiber fineness, but not with other characteristics.

Inspired by the literature, we develop a new ecoepidemiological model that uses differential equations to investigate and analyze the dynamics of the cotton leaf curl virus (CLCuV) of cotton plants. Moreover, our present model is unique in that it divides the cotton leaf curl virus (CLCuV) model into cotton and vector populations. Cotton and vector populations both have susceptible and infected subclasses. The findings of our study are useful in developing effective methods for preventing or eradicating the spread of a cotton leaf curl virus disease. This research is structured as follows. Part two involves the development of a novel mathematical model for the transmission dynamics of cotton leaf curl virus (CLCuV). The existence and stability of cotton leaf curl virus (CLCuV) equilibria, as well as the positivity and boundedness of solutions, are discussed in part three. Part four addresses numerical simulation. Part five concludes with conclusions.

2. Model Formulation

In this section, we divided the cotton leaf curl virus (CLCuV) model into cotton and vector populations. We considered the susceptible and infected subgroups of these populations. $A(t)$ represents susceptible cotton, and $B(t)$ represents infected cotton. Similarly, $C(t)$ represents the susceptible vector, and $D(t)$ represents the infected vector. The model assumed recruitment rate of susceptible vectors by k_2 and moves to infected vectors (D) with ω_2 rate after consuming ill plants or cotton. The susceptible cotton (A) also replanted at rate k_1 and the diseases spread to cotton, when infected vectors (D) react with susceptible cotton (A) at rate of ω_1 through eating. Cotton once become infected not ever mends and gives yield or produce very low yield of cotton. The model also assumes that α is the natural death rate for cotton population and β is natural death rate for vector population. All the descriptions of the parameters are listed in Table 1.

Using the assumptions and flow chart of the model in Figure 1, we can derive the following nonlinear ordinary differential equations:

$$\frac{dA}{dt} = k_1 - \omega_1 AD - \alpha A, \tag{1}$$

$$\frac{dB}{dt} = \omega_1 AD - \alpha B, \tag{2}$$

$$\frac{dC}{dt} = k_2 - \omega_2 BC - \beta C, \tag{3}$$

Table 1: Parameters of the model.

Parameter	Description
k_1	Replanting rate of cotton
k_2	Recruitment rate of vector
ω_1	Infection rate of cotton
ω_2	Infection rate of vector
α	Natural death rate of cotton
β	Natural death rate of vector

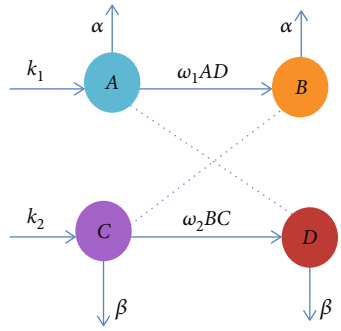

Figure 1: Flow chart of the model.

$$\frac{dD}{dt} = \omega_2 BC - \beta D, \tag{4}$$

with

$$A(0) = A_0 > 0, B(0) = B_0 \geq 0, C(0) = C_0 \geq 0, D(0) = D_0 \geq 0. \tag{5}$$

3. Model Analysis

3.1. Positivity of Solution. In this subsection, our model (Equations (1), (2), (3), and (4)) to be ecoepidemiologically meaningful and well posed, it is necessary to prove that all state variables of system with positive initial data will remain positive for all times $t \geq 0$. The following theorem is used to demonstrate the positivity of the system of Equations (1), (2), (3), and (4).

Theorem 1. *Let* $\Omega = \{(A, B, C, D) \in \mathbf{R}^4 : A(0) > 0, B(0) > 0, C(0) >, D(0) > 0\}$. *Then, the solution set* $\{A(t), B(t), C(t), D(t)\}$ *of system of Equations (1), (2), (3), and (4) are positive for all* $t \geq 0$.

Proof. From the first equation of system Equations (1), (2), (3), and (4), we have that

$$\frac{dA}{dt} = k_1 - (\omega_1 D + \alpha)A \geq -(\omega_1 D + \alpha)A. \tag{6}$$

Using separation variables and by integrating Equation (6)

$$\begin{aligned} \int \frac{dA}{A} &\geq -\int (\omega_1 D + \alpha)dt, \\ lnA(t) &\geq -\int (\omega_1 D + \alpha)dt + c_1, \\ A(t) &\geq e^{-\int (\omega_1 D + \alpha)dt + c_1}, \\ A(t) &\geq A(0)e^{-\int (\omega_1 D + \alpha)dt} > 0. \end{aligned} \tag{7}$$

From the second equation of system Equations (1), (2), (3), and (4), we have that:

$$\frac{dB}{dt} = \omega_1 AD - \alpha B \geq -\alpha B. \tag{8}$$

Using separation variables and by integrating Equation (8)

$$\begin{aligned} \int \frac{dB}{B} &\geq -\int \alpha dt, \\ lnB(t) &\geq -\alpha t + c_2, \\ B(t) &\geq e^{-\alpha t + c_2}, \\ B(t) &\geq B(0)e^{-\alpha t} \geq 0. \end{aligned} \tag{9}$$

Furthermore, using similar procedure on the above, we have

$$\begin{aligned} C(t) &\geq C(0)e^{-\int (\omega_2 B + \beta)dt} \geq 0, \\ D(t) &\geq D(0)e^{-\beta t} \geq 0. \end{aligned} \tag{10}$$

Hence, all the solution sets are positive for $t \geq 0$, that is the model is meaningful and well posed. □

3.2. Invariant Region. We determine a region in which the solution of system of Equations (1), (2), (3), and (4) are bounded. Now, differentiating the total cotton population, $N_c = A + B$ with respect to time, we have

$$\frac{dN_c}{dt} = k_1 - \alpha N_c. \tag{11}$$

By re-arranging and multiplying Equation (11) by integrating factor $e^{\int \alpha dt} = e^{\alpha t}$, we have

$$\frac{dN_c}{dt} e^{\alpha t} + \alpha N_c e^{\alpha t} = k_1 e^{\alpha t}. \tag{12}$$

That is

$$\frac{d}{dt}\left(N_c e^{\alpha t}\right) = k_1 e^{\alpha t}. \tag{13}$$

By integrating and solving Equation (13), we obtain

$$N_c(t) = \frac{k_1}{\alpha} + e^{-\alpha t}\left(N_c(0) - \frac{k_1}{\alpha}\right). \tag{14}$$

Taking the limit as $t \longrightarrow \infty$ to Equation (14), we obtain

$$\Omega_c = \left\{ (A, B) \in R_+^2 : N_c \leq \frac{k_1}{\alpha} \right\}. \tag{15}$$

And differentiating the cotton leaf curl virus population, $N_v = C + D$, we have

$$\frac{dN_v}{dt} = k_2 - \beta N_v. \tag{16}$$

Using similar procedure on the above

$$N_v(t) = \frac{k_2}{\beta} + e^{-\beta t}\left(N_v(0) - \frac{k_2}{\beta}\right). \tag{17}$$

Taking the limit as $t \longrightarrow \infty$ to Equation (17), we obtain

$$\Omega_v = \left\{ (C, D) \in R_+^2 : N_v \leq \frac{k_2}{\beta} \right\}. \tag{18}$$

As a result, the feasible solution set for the CLCuV model is given by:

$$\Omega = \Omega_c \times \Omega_v = \left\{ (A, B, C, D) \in R_+^4 : N_c \leq \frac{k_1}{\alpha} : N_v \leq \frac{k_2}{\beta} \right\} \tag{19}$$

that is positively invariant inside in which the model is considered to be ecoepidemiologically meaningful and mathematically well posed.

3.3. Disease Free Equilibrium Point of the Model. The model's disease-free equilibrium points, E_0, are stationary solutions in which there is no infection. It is obtained by equating Equations (1), (2), (3), and (4) to zero and using $B = 0$ and $D = 0$. Then, disease free equilibrium point, E_0 of our model Equation (1) is given by

$$E_0 = \left(A^0, B^0, C^0, D^0\right) = \left(\frac{k_1}{\alpha}, 0, \frac{k_2}{\beta}, 0\right). \tag{20}$$

The basic reproduction number R_0: The basic reproduction number, R_0, quantifies the predicted number of secondary infections caused by a single newly infected individual delivered directly into a susceptible group (Kinene et al. [22]). By rewriting the system of Equations (1), (2), (3), and (4) starting with newly infective classes and using the next generation matrix method, the basic reproduction number R_0 can be obtained as

$$\begin{aligned} \frac{dB}{dt} &= \omega_1 AD - \alpha B, \\ \frac{dD}{dt} &= \omega_2 BC - \beta D. \end{aligned} \tag{21}$$

Then, we consider

$$f = \begin{pmatrix} \omega_1 AD \\ \omega_2 BC \end{pmatrix}, \nu = \begin{pmatrix} \alpha B \\ \beta D \end{pmatrix}. \tag{22}$$

Now, the Jacobian matrix of f and ν with respect to B and D at disease free equilibrium point, $E_0 = ((k_1/\alpha), 0, (k_2/\beta), 0)$, is

$$F = \begin{pmatrix} 0 & \dfrac{\omega_1 k_1}{\alpha} \\ \dfrac{\omega_2 k_2}{\beta} & 0 \end{pmatrix}, V = \begin{pmatrix} \alpha & 0 \\ 0 & \beta \end{pmatrix}. \tag{23}$$

Then, by the principle of next generation matrix, the basic reproduction number R_0 is the dominant eigen value of the FV^{-1} or spectral radius of FV^{-1} where

$$FV^{-1} = \begin{pmatrix} 0 & \dfrac{\omega_1 k_1}{\alpha} \\ \dfrac{\omega_2 k_2}{\beta} & 0 \end{pmatrix} \begin{pmatrix} \dfrac{1}{\alpha} & 0 \\ 0 & \dfrac{1}{\beta} \end{pmatrix} = \begin{pmatrix} 0 & \dfrac{\omega_1 k_1}{\alpha\beta} \\ \dfrac{\omega_2 k_2}{\beta\alpha} & 0 \end{pmatrix}. \tag{24}$$

The characteristic equations of Equation (24) becomes

$$\lambda^2 - \frac{k_1 k_2 \omega_1 \omega_2}{\alpha^2 \beta^2} = 0. \tag{25}$$

That is

$$\lambda = \pm\sqrt{\frac{k_1 k_2 \omega_1 \omega_2}{\alpha^2 \beta^2}}. \tag{26}$$

Since, basic reproduction number R_0 is the maximum eigen values of FV^{-1} or the spectral radius of FV^{-1}. As a result,

$$R_0 = \sqrt{\frac{k_1 k_2 \omega_1 \omega_2}{\alpha^2 \beta^2}}. \tag{27}$$

The two generation are required to transmission of CLCuV to take place in the cotton field that is from an infectious cotton plant to susceptible vector and then from an infectious vector to susceptible cotton (Van den Driessche and Watmough [23]). That is why the square root found in R_0. It implies that

$$R_0 = \sqrt{\frac{k_1 k_2 \omega_1 \omega_2}{\alpha^2 \beta^2}} = \sqrt{\frac{k_1 \omega_1}{\alpha^2}\frac{k_2 \omega_2}{\beta^2}} = \sqrt{\frac{k_1 \omega_1}{\alpha^2}}\sqrt{\frac{k_2 \omega_2}{\beta^2}} = R_{0c} \times R_{0v}. \tag{28}$$

where $R_{0c} = \sqrt{k_1\omega_1/\alpha^2}$ is the cotton plants contribution when they infect the vector and $R_{0v} = \sqrt{k_2\omega_2/\alpha^2}$ is the contribution of the vector population when it infects cotton plants.

3.4. Local Stability of the Disease Free Equilibrium Point. The linearization system of Equations (1), (2), (3), and (4) at E_0 can be used to find the local stability of the model at disease-free equilibrium point, E_0.

Theorem 2. *Disease free equilibrium point, E_0 of system of Equations (1), (2), (3), and (4) are locally asymptotically stable, if $R_0 < 1$.*

Proof. The Jacobian matrix of system of Equations (1), (2), (3), and (4) is

$$J = \begin{pmatrix} -(\omega_1 D + \alpha) & 0 & 0 & -\omega_1 A \\ \omega_1 D & -\alpha & 0 & \omega_1 A \\ 0 & -\omega_2 C & -(\omega_2 B + \beta) & 0 \\ 0 & \omega_2 C & \omega_2 B & -\beta \end{pmatrix}. \tag{29}$$

Evaluating the Jacobian matrix of system of Equation (29) at disease free equilibrium point $E_0 = (k_1/\alpha, 0, k_2/\beta, 0)$ is

$$J(E_0) = \begin{pmatrix} -\alpha & 0 & 0 & -\dfrac{\omega_1 k_1}{\alpha} \\ 0 & -\alpha & 0 & \dfrac{\omega_1 l_1}{\alpha} \\ 0 & -\dfrac{\omega_2 k_2}{\beta} & -\beta & 0 \\ 0 & \dfrac{\omega_2 k_2}{\beta} & 0 & -\beta \end{pmatrix}. \tag{30}$$

The characteristic equation of Jacobian matrix of Equation (30) at disease free equilibrium point, E_0, is $|J(E_0) - \lambda I_4| = 0$. That is

$$\begin{vmatrix} -\alpha - \lambda & 0 & 0 & -\dfrac{\omega_1 k_1}{\alpha} \\ 0 & -\alpha - \lambda & 0 & \dfrac{\omega_1 k_1}{\alpha} \\ 0 & -\dfrac{\omega_2 k_2}{\beta} & -\beta - \lambda & 0 \\ 0 & \dfrac{\omega_2 k_2}{\beta} & 0 & -\beta - \lambda \end{vmatrix} = 0. \tag{31}$$

Evaluating Equation (31) simplifying it, we get

$$(-\alpha - \lambda)(-\beta - \lambda)\left(\lambda^2 + d_1\lambda + d_2\right) = 0, \tag{32}$$

where

$$\begin{aligned} d_1 &= \alpha + \beta, \\ d_2 &= \alpha\beta - \frac{k_1 k_2 \omega_1 \omega_2}{\alpha\beta} = \alpha\beta\left[1 - \frac{k_1 k_2 \omega_1 \omega_2}{\alpha^2\beta^2}\right] = \alpha\beta\left(1 - R_0^2\right). \end{aligned} \tag{33}$$

Clearly, from Equation (32), we observe that

$$\begin{aligned} \lambda_1 &= -\alpha < 0, \\ \lambda_2 &= -\beta < 0, \end{aligned} \tag{34}$$

and from the last expression of Equation (32), that is

$$\lambda^2 + d_1\lambda + d_2 = 0, \tag{35}$$

By using the Routh-Hurwitz criteria, Equation (35) has strictly a negative real root if $d_1 > 0$ and $d_2 > 0$. Clearly, we observe that $d_1 = \alpha + \beta > 0$ and

$$d_2 = \alpha\beta\left(1 - R_0^2\right) > 0, \tag{36}$$

if $(1 - R_0^2) > 0$. That is, $R_0^2 < 1$ implies that $R_0 < 1$. As a result, our model Equations (1), (2), (3), and (4) at E_0 offers all eigenvalues with a negative real part, and so it is locally asymptotically stable if $R_0 < 1$. □

3.5. Global Stability of the Disease Free Equilibrium Point. To establish the global stability of the disease free equilibrium point E_0, we use the method proposed by Castillo-Chavez et al. [24] and Fantaye and Birhanu [25]. Based on these, we have written the system of Equations (1), (2), (3), and (4) in the following form:

$$\frac{dM}{dt} = J(M, L), \tag{37}$$

$$\frac{dL}{dt} = P(M, L), \tag{38}$$

$$P(M, 0) = 0, \tag{39}$$

where $M = (A, C) \in R^2$ represent the number of uninfected classes, while $L = (B, D) \in R^2$ represent the number of infected classes and $E_0 = (M^*, 0)$ represents the disease-free equilibrium of this system. The disease-free equilibrium E_0 is globally asymptotically stable equilibrium for the model if the following conditions are fulfilled:

(1) $dM/dt = J(M, 0), M^*$ is globally asymptotically stable:

$$\frac{dL}{dt} = D_L P(M^*, 0)L - \widehat{P}(M, L), \widehat{P}(M, L) \geq 0 \forall (M, L) \in \Omega, \tag{40}$$

where $D_L P(M^*, 0)$ is an M-matrix and $P(M, L)$ taken in (B, D) and evaluated at $(M^*, 0) = (k_1/\alpha, k_2/\beta, 0, 0)$. If system of Equation (37) satisfies the above conditions, then the following theorem holds.

Theorem 3. *The disease free equilibrium point, $E_0 = (M^*, 0)$ of system of Equation (37) is globally asymptotically stable if $R_0 \leq 1$, and Conditions (1) and (5) are holds.*

Proof. From our model of Equations (1), (2), (3), and (4), we can obtain $J(M, L)$ and $P(M, L)$:

$$J(M,L) = \begin{pmatrix} k_1 - \omega_1 AD - \alpha A \\ k_2 - \omega_2 BC - \beta C \end{pmatrix}, \quad P(M,L) = \begin{pmatrix} \omega_1 AD - \alpha B \\ \omega_2 BC - \beta D \end{pmatrix}. \tag{41}$$

Now, we consider the reduced system $dM/dt = J(M, 0)$ from Condition (1):

$$\frac{dA}{dt} = k_1 - \alpha A, \tag{42}$$

$$\frac{dC}{dt} = k_2 - \beta C. \tag{43}$$

$M^* = (k_1/\alpha, k_2/\beta)$ is a globally asymptotically stable equilibrium point for the reduced system $dM/dt = J(M, 0)$. This can be verifed from the solution of Equation (42); we get $A(t) = (k_1/\alpha) + (A(0) - (k_1/\alpha))e^{-\alpha t}$ which approaches k_1/α as $t \longrightarrow \infty$, and from Equation (43), we obtain $C(t) = (k_2/\beta(k_2/\beta)) + (C(0) - (k_2/\beta(k_2/\beta)))e^{-\beta t}$ which approaches k_2/β as $t \longrightarrow \infty$, We note that this asymptomatic dynamics is independent of the initial conditions in Ω; therefore, the convergence of the solutions of the reduced system (42) and (43) is global in Ω. Now, we compute

$$D_L P(M^*, 0) = \begin{pmatrix} -\alpha & \dfrac{k_1\omega_1}{\alpha} \\ \dfrac{k_2\omega_2}{\beta} & -\beta \end{pmatrix}. \tag{44}$$

Then, $P(M, L)$ can be written as

$$P(M, L) = D_L P(M^*, 0)L - \widehat{P}(M, L), \tag{45}$$

and we want to show $\widehat{P}(M, L)$, which is obtained as

$$\widehat{P}(M,L) = \begin{pmatrix} \omega_1 D\left(\dfrac{k_1}{\alpha} - A\right) \\ \omega_2 B\left(\dfrac{k_2}{\beta} - C\right) \end{pmatrix}. \tag{46}$$

Here $(k_1/\alpha(k_1/\alpha)) \geq A$ and $((k_2/\beta)k_2/\beta) \geq B$. Hence, it is clear that $\widehat{P}(M, L) \geq 0$, $\forall (M, L) \in \Omega$. Thus, this proves that disease free equilibrium point E_0 is globally asymptotically stable when $R_0 \leq 1$. □

3.6. Disease Endemic Equilibrium Point of the Model. The endemic equilibrium point, E_1, of the model is the steady state solution where leaf curl virus persist in the population of cotton plants. We can obtain by equating each system of the equation equal to zero; that is,

$$k_1 - \omega_1 A^* D^* - \alpha A^* = 0, \tag{47}$$

$$\omega_1 A^* D^* - \alpha B^* = 0, \tag{48}$$

$$k_2 - \omega_2 B^* C^* - \beta C^* = 0, \tag{49}$$

$$\omega_2 B^* C^* - \beta D^* = 0, \tag{50}$$

From first equation of (47), we get

$$A^* = \frac{k_1}{\omega_1 D^* + \alpha}. \tag{51}$$

From second equation of (47), we have

$$B^* = \frac{\omega_1 A^* D^*}{\alpha}. \tag{52}$$

Substituting the value of A^* from Equation (51) into Equation (52), we obtain

$$B^* = \frac{k_1\omega_1 D^*}{\alpha(\omega_1 D^* + \mu)}. \tag{53}$$

From third equation of (47), we have

$$C^* = \frac{k_2}{\omega_2 B^* + \beta}. \tag{54}$$

Substituting the value of B^* from Equation (53) into Equation (54), we obtain

$$C^* = \frac{k_2\alpha(\omega_1 D^* + \alpha)}{k_1\omega_1\omega_2 D^* + \beta\alpha(\omega_1 D^* + \alpha)}. \tag{55}$$

From the last Equation (47), we have

$$\omega_2 B^* C^* = \beta D^*. \tag{56}$$

Substituting the value B^* from Equation (53) and the value C^* from Equation (55) in Equation (56), we have

$$\frac{k_1 k_2 \omega_1 \omega_2}{k_1\omega_1\omega_2 D^* + \beta\alpha(\omega_1 D^* + \alpha)} = \beta. \tag{57}$$

By re-arranging and simplifying Equation (57), we get

$$D^* = \frac{\alpha^2\beta\left(R_0^2 - 1\right)}{\omega_1(k_1\omega_2 + \alpha\beta)}. \tag{58}$$

Thus, by substituting Equation (58) into Equations (51), (53), and (55), we obtain

$$A^* = \frac{k_1(k_1\omega_2 + \alpha\beta)}{\alpha^2\beta\left(R_0^2 - 1\right) + \alpha(k_1\omega_2 + \alpha\beta)},$$
$$B^* = \frac{k_1\beta\left(R_0^2 - 1\right)}{\alpha\beta\left(R_0^2 - 1\right) + (k_1\omega_2 + \alpha\beta)},$$
$$C^* = \frac{k_2\left(\alpha\beta\left(R_0^2 - 1\right) + k_1\omega_2 + \alpha\beta\right)}{\beta\left((k_1\omega_2 + \alpha\beta)\left(R_0^2 - 1\right) + k_1\omega_2 + \alpha\beta\right)}. \tag{59}$$

3.7. Local Stability of the Endemic Equilibrium Point. In this part, we use the Jacobian stability approach to demonstrate the local stability of the disease endemic equilibrium condition.

Theorem 4. *When $R_0 > 1$, the model's endemic equilibrium point, E_1, is locally asymptotically stable.*

Proof. The local stability of the endemic equilibrium, E_1, is determined based on the signs of the eigenvalues of the Jacobian matrix which is computed at the disease endemic equilibrium, E_1. Now, the Jacobian matrix of the model at E_1 is given by

$$J = \begin{pmatrix} -(\omega_1 D^* + \alpha) & 0 & 0 & -\omega_1 A^* \\ \omega_1 D^* & -\alpha & 0 & \omega_1 A^* \\ 0 & -\omega_2 C^* & -(\omega_2 B^* + \beta) & 0 \\ 0 & \omega_2 C^* & \omega_2 B^* & -\beta \end{pmatrix}. \tag{60}$$

The characteristic equation of Jacobian matrix of Equation (60) at disease endemic equilibrium point, E_1, is $|J(E_1) - \lambda I_4| = 0$. That is:

$$\begin{vmatrix} -(\omega_1 D^* + \alpha) - \lambda & 0 & 0 & -\omega_1 A^* \\ \omega_1 D^* & -\alpha - \lambda & 0 & \omega_1 A^* \\ 0 & -\omega_2 C^* & -(\omega_2 B^* + \beta) - \lambda & 0 \\ 0 & \omega_2 C^* & \omega_2 B^* & -\beta - \lambda \end{vmatrix} = 0. \tag{61}$$

Equation (61) can be simplified as

$$P(\lambda) = f_4\lambda^4 + f_3\lambda^3 + f_2\lambda^2 + f_1\lambda + f_0, \tag{62}$$

where

$$f_4 = 1, f_3 = 2\alpha + 2\beta + \omega_1 D^* + \omega_2 B^*,$$
$$f_2 = \alpha\beta + (\alpha + \beta)(\alpha + \beta)\alpha)\beta + (2\beta + \alpha)\omega_1 D^* + (2\alpha + \beta)\omega_2 B^* + \omega_1\omega_2(B^* - A^* C^*),$$
$$f_1 = \mu\beta(\alpha + \beta) + (\alpha + \beta)\alpha\beta + (\alpha\beta + (\alpha + \beta)\alpha)\omega_2 B^* + (\alpha + \beta))\beta\omega_1)D^* + (\alpha + \beta)\omega_1\omega_2 B^* D^* - \omega_1\omega_2(\alpha + \beta)A^* C^*,$$
$$f_0 = \beta\omega_1\omega_2\alpha B^* D^* + \omega_1\beta^2\alpha D^* + \beta\alpha\omega_2\alpha B^* + \alpha^2\beta^2 - \alpha\beta\omega_1\omega_2 A^* C^*. \tag{63}$$

Now, the characteristic polynomial of Equation (62) can be analyzed by Routh-Hurwitz criteria. The coefficients f_4, f_3, f_2, f_1, f_0 of the characteristic polynomial are real positive. As a result, the necessary criterion for the disease endemic equilibrium point's stability is met. The adequate condition for system stability using the Hurwitz array for the characteristic polynomial is then provided as follows:

$$\begin{array}{c|ccc} s^4 & \mathrm{f}_4 & \mathrm{f}_2 & \mathrm{f}_0 \\ s^3 & \mathrm{f}_3 & \mathrm{f}_1 & 0 \\ s^2 & \mathrm{g}_1 & \mathrm{g}_2 & \mathrm{g}_3 \\ s^1 & \mathrm{h}_1 & \mathrm{h}_2 & \mathrm{h}_3 \\ s^0 & \mathrm{k}_1 & \mathrm{k}_2 & \mathrm{k}_3 \end{array}, \tag{64}$$

where f_4, f_3, f_2, f_1, f_0 are the coefficients of the characteristic polynomial and the remaining elements in the array are obtained as follows:

$$g_1 = -\frac{1}{f_3}\begin{vmatrix} f_4 & f_2 \\ f_3 & f_1 \end{vmatrix} = \frac{f_3 f_2 - f_1}{f_3} > 0,$$
$$g_2 = -\frac{1}{f_3}\begin{vmatrix} f_4 & f_0 \\ f_3 & 0 \end{vmatrix} = f_0,$$
$$g_3 = -\frac{1}{f_3}\begin{vmatrix} f_4 & 0 \\ f_3 & 0 \end{vmatrix} = 0,$$
$$h_1 = -\frac{1}{g_1}\begin{vmatrix} f_3 & f_1 \\ g_1 & g_2 \end{vmatrix} = \frac{f_1 g_1 - f_3 f_0}{g_1} > 0,$$
$$h_2 = -\frac{1}{g_1}\begin{vmatrix} f_3 & 0 \\ g_1 & 0 \end{vmatrix} = 0,$$
$$h_3 = -\frac{1}{g_1}\begin{vmatrix} f_3 & 0 \\ g_1 & 0 \end{vmatrix} = 0,$$
$$k_1 = -\frac{1}{h_1}\begin{vmatrix} g_1 & g_2 \\ h_1 & 0 \end{vmatrix} = f_0,$$
$$k_2 = -\frac{1}{h_1}\begin{vmatrix} g_1 & 0 \\ h_1 & 0 \end{vmatrix} = 0,$$
$$k_3 = -\frac{1}{h_1}\begin{vmatrix} g_1 & 0 \\ h_1 & 0 \end{vmatrix} = 0. \tag{65}$$

Since the coefficients of the characteristic polynomial, f_4, f_3, f_2, f_1, f_0 are real positive, and the first column of the Routh-Hurwitz array has the same positive sign. Therefore, by using the Routh-Hurwitz criteria, all eigenvalues of the characteristics polynomial are negative. Thus, the disease endemic equilibrium point E_1 is locally asymptotically stable if $R_0 > 1$. □

3.8. Global Stability of Disease Endemic Equilibrium Point

Theorem 5. *For $R_0 > 1$, then the system of Equations (1), (2), (3), and (4) at E_1 is globally asymptotical stable.*

Proof. To investigate the global stability of the endemic equilibrium point E_1, we consider the following Lyapunov function for model of Equations (1), (2), (3), and (4):

$$V(t) = K_1 \frac{(A - A^*)^2}{2} + K_2 \frac{(B - B^*)^2}{2} + K_3 \frac{(C - C^*)^2}{2} + K_4 \frac{(D - D^*)^2}{2}, \tag{66}$$

where K_1, K_2, K_3, K_4 are chosen. By differentiating (66) with respect to time, we have

$$\frac{dV}{dt} = K_1(A - A^*)\frac{dA}{dt} + K_2(B - B^*)\frac{dB}{dt} + K_3(C - C^*)\frac{dC}{dt} + K_4(D - D^*)\frac{dD}{dt}. \tag{67}$$

Using system Equations (1), (2), (3), and (4), Equation (67) can becomes

$$\begin{aligned}\frac{dV}{dt} = {} & K_1(A - A^*)[k_1 - (\omega_1 D + \alpha)A] \\ & + K_2(B - B^*)[\omega_1 AD - \alpha B] \\ & + K_3(C - C^*)[k_2 - (\omega_2 B + \beta)C] \\ & + K_4(D - D^*)[\omega_2 BC - \beta D].\end{aligned} \tag{68}$$

By re arranging Equation (68), we have

$$\begin{aligned}\frac{dV}{dt} = {} & -K_1(A - A^*)A\left[-\frac{k_1}{A} + (\omega_1 D + \alpha)\right] \\ & - K_2(B - B^*)B\left[-\frac{\omega_1 AD}{B} + \alpha\right] \\ & - K_3(C - C^*)C\left[-\frac{k_2}{C} + (\omega_2 B + \beta)\right] \\ & - K_4(D - D^*)D\left[-\frac{\omega_2 BC}{D} + \beta\right].\end{aligned} \tag{69}$$

Table 2: The parameter values and sensitivity index of model.

Parameter	Value	Sensitivity index
k_1	0.97	+ve
k_2	0.27	+ve
ω_1	0.000007	+ve
ω_2	0.000005	+ve
α	0.04	-ve
β	0.03	-ve

Here, we can choose

$$\begin{aligned}K_1 &= \frac{A}{(\omega_1 D + \mu)A - k_1}, \\ K_2 &= \frac{B}{\alpha B - \omega_1 AD}, \\ K_3 &= \frac{C}{(\omega_2 B + \beta)C - k_2} \\ K_4 &= \frac{D}{\beta D - \omega_2 BC}.\end{aligned} \tag{70}$$

Hence, we observe that $dV/dt < 0$ and an endemic equilibrium point, E_1, of the model is globally stable. Moreover, $dV/dt = 0$ if and only if either $A = A^*, B = B^*, C - C^*, D - D^*$ or $A = B = C = D = 0$. Thus, using LaSalle [26], E_1 is global asymptotical stable whenever $R_0 > 1$. □

3.9. Sensitivity Analysis of Model Parameters. In order to establish the robustness of model predictions, sensitivity analysis is widely used to test and discover parameters that can alter the basic reproduction number, R_0. It demonstrates the significance of each parameter in disease transmission. Sensitivity indices measure how much a variable changes when a parameter is altered Rodrigues et al. [27]. When the variable is a differentiable function of the parameter, then the sensitivity index can also be calculated using partial derivatives.

Definition 6. The normalized forward sensitivity index of a R_0 that depends differentiably on a parameter, x_i, is given as

$$\Pi_{x_i}^{R_0} = \frac{\partial R_0}{\partial x_i} \cdot \frac{x_i}{R_0}, \tag{71}$$

where x_i represent all the basic parameters. For example,

$$\begin{aligned}M_{k_1}^{R_0} &= \frac{\partial R_0}{\partial k_1} \cdot \frac{k_1}{R_0}, \\ &= \left(\frac{1}{2\sqrt{(k_1 b_2 \omega_1 \omega_2)/(\alpha^2 \beta^2)}} \frac{k_2 \omega_1 \omega_2}{\alpha^2 \beta^2}\right) \\ &\quad \cdot \frac{k_1}{\sqrt{(k_1 b_2 \omega_1 \omega_2)/(\alpha^2 \beta^2)}}, = \frac{1}{2}.\end{aligned} \tag{72}$$

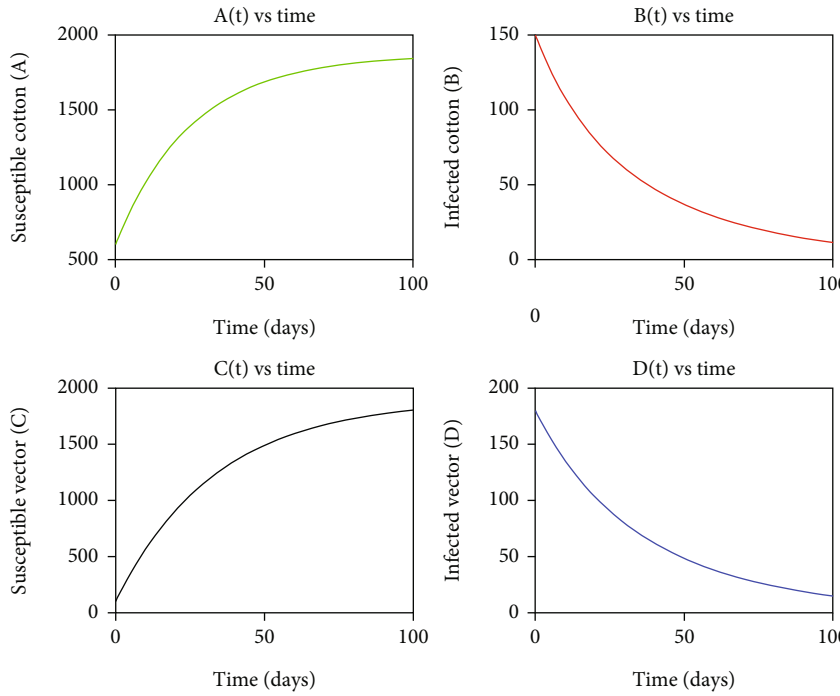

Figure 2: Time series plot of state variables for $R_0 = 0.3223 < 1$.

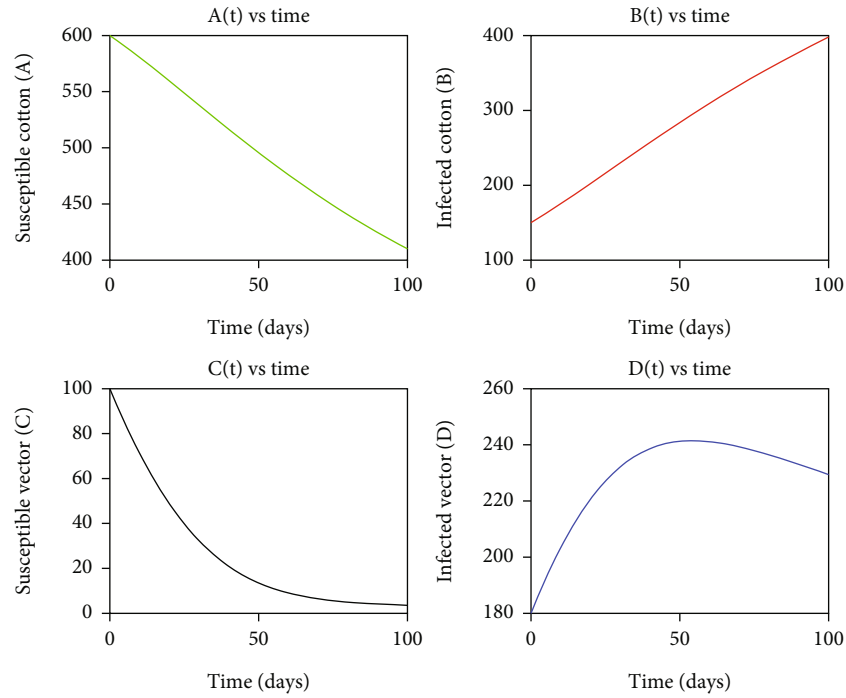

Figure 3: Time series plot of state variables for $R_0 = 24.5286 > 1$

Using the same method, we calculate the sensitivity indexes for the other parameters. Table 2 presents the criteria in decreasing order of sensitivity.

3.10. Interpretation of Sensitivity Indices. Table 2 displays the sensitivity indices of the basic reproductive number in relation to the important parameters. Positive indices $(k_1, k_1, \omega_1, \text{and } \omega_2)$ indicate that parameters with increasing values have a significant impact on the spread of the disease. Since the basic reproduction number rises as their values rise, so does the average number of secondary cases of infection. Additionally, those parameters with negative sensitivity indices (α, β) have the effect of reducing disease burden when their values rise, while the others remain constant.

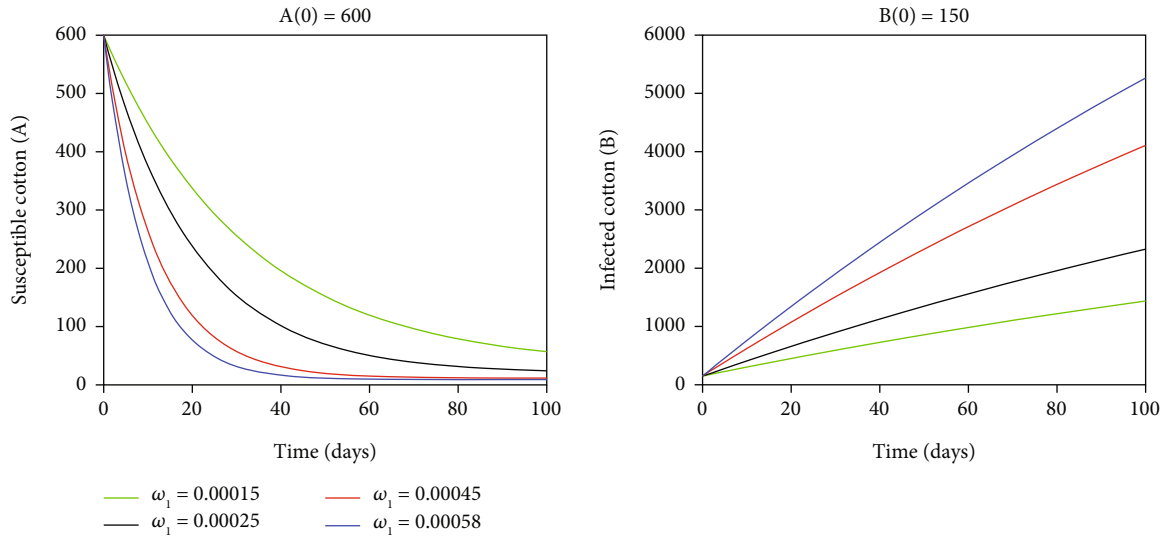

Figure 4: Susceptible cotton population (A) and infected cotton population (B) w.r.t. time t for different values of ω_1.

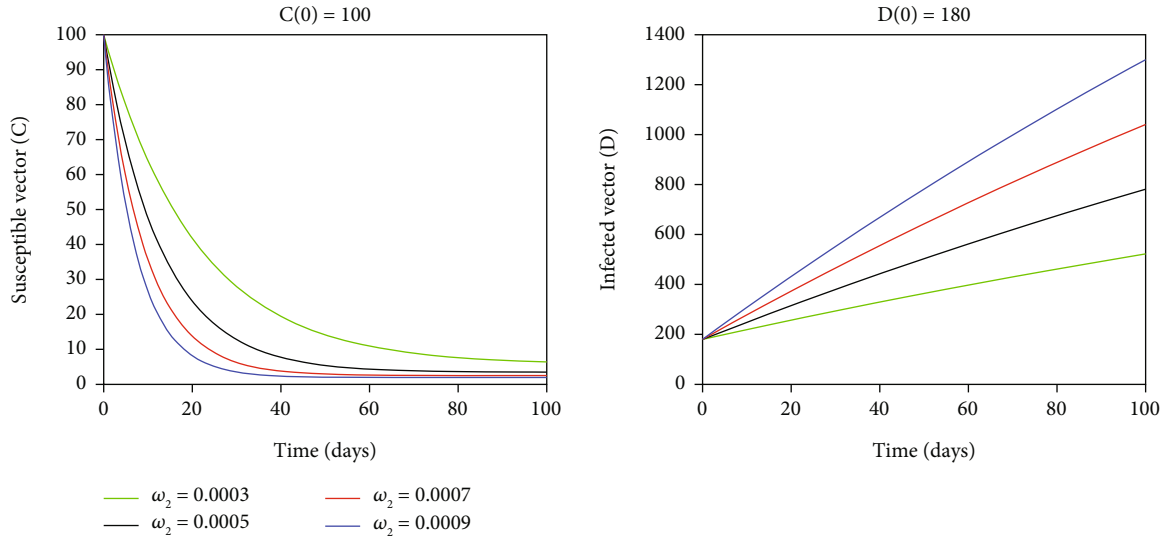

Figure 5: Susceptible vector population (C) and infected vector population (D) w.r.t. time t for different values of ω_2.

Additionally, as their values rise, the basic reproduction number falls, resulting in a reduction in the disease's endemic areas.

4. Numerical Simulation

In this section, we use MATLAB ode45 solvers to numerically validate our work. The simulations investigate the effect of different model parameter combinations on the transmission dynamics of cotton leaf curl virus (CLCuV). The simulation was performed using a variety of parameter values. The source of the collection of parameter values is mostly based on assumptions. The relevant initial circumstances are used in the simulations and analyses: $A(0) = 600, B(0) = 150, C(0) = 100, D(0) = 180$, and the parameters values are displayed in Table 2.

The time series plot of state variables for $R_0 < 1$ and $R_0 > 1$ is shown in Figures 2 and 3. Figure 2 shows that susceptible cotton begins to rise asymptotically to the disease free equilibrium point, whereas infected cotton populations drop asymptotically to the disease free equilibrium point. Furthermore, the susceptible vector population grows asymptotically to the disease free equilibrium point, but the infected vector population falls asymptotically to the disease free equilibrium point. In this situation, the disease may eventually eliminate in the long run. The existence of such condition is due to the fact that $R_0 = 0.3223$ which is less than one. This supports the theorem that the stability of disease free equilibrium point exists when $R_0 < 1$, that is, if $R_0 < 1$, then on average, one infected cotton plant produces less than one newly infectious plant over the course of its disease period.

Figure 3 shows that susceptible cotton and vector individuals are reduced due to the influence of infected cotton

and vector individuals, after which they join the infected class, resulting in an increase in infected cotton and vector people. As a result, there is an increase in infected cotton and vectors, and the disease endemic equilibrium point exists and is stable. The existence of this condition is due to the fact that $R_0 = 24.5286$ which is greater than one. This supports the theorem that the stability of disease endemic equilibrium point exists when $R_0 > 1$, that is, if $R_0 > 1$, each infected cotton and vectors produces, on average more than one new infected cotton and vectors, then disease will be able to spread in the given area.

Susceptible cotton population (A) and infected cotton population (B) with respect to time t for different values of ω_1 are shown in Figure 4. From Figure 4, we observe that as infection rate of cotton, ω_1, increases, susceptible cotton population (A) decreases, while infected cotton population (B) increased. Also, susceptible vector population (C) and infected vector population (D) with respect to time t for different values of ω_2 are shown in Figure 5. From Figure 5, we observe that as the value of infection rate of vector, ω_2, increases, susceptible vector population (C) decreases, while infected vector population (D) increased.

5. Conclusion

In this study, an ecoepidemiological model for the transmission dynamics of cotton leaf curl virus (CLCuV) disease in cotton plant was developed. The model's well-posedness, positivity, and boundedness are all explored. The basic reproduction number and the stability analysis of the model's cotton equilibria were investigated. According to the study, if the basic reproduction number is less than one, the cotton-free equilibrium is locally and globally asymptotically stable; however, if the basic reproduction number is more than one, the endemic equilibrium is locally asymptotically stable. The numerical simulation shows that as infection rate of cotton, ω_1, increases, susceptible cotton population (A) decreases, while infected cotton population (B) increased. Furthermore, as the value of infection rate of vector, ω_2, increases, susceptible vector population (C) decreases, while infected vector population (D) increased. Optimal control and the cost-effectiveness analysis of the integrated strategy would be considered in a future study.

Data Availability

The data supporting this nonlinear ecoepidemiological model are taken using assumption which are relevant to this paper.

Conflicts of Interest

The authors declare that they have no conflicts of interest.

References

[1] D. Monga and S. Sain, "Incidence and severity of cotton leaf curl virus disease on different bg ii hybrids and its effect on the yield and quality of cotton crop," *Journal of Environmental Biology*, vol. 42, no. 1, pp. 90–98, 2021.

[2] S. Vanitha, "Decision support model for prioritization of cotton plant diseases using integrated fahp-topsis approach," *Turkish Journal of Computer and Mathematics Education (TURCOMAT)*, vol. 12, no. 10, pp. 7488–7496, 2021.

[3] S. K. Sain, D. Monga, M. Mohan, A. Sharma, and J. Beniwal, "Reduction in seed cotton yield corresponding with symptom severity grades of cotton leaf curl disease (clcud) in upland cotton (gossypium hirsutum l.)," *International Journal of Current Microbiology and Applied Sciences*, vol. 9, no. 11, pp. 3063–3076, 2020.

[4] Z. Zhang, J. Rong, V. N. Waghmare et al., "Qtl alleles for improved fiber quality from a wild Hawaiian cotton, gossypium tomentosum," *Theoretical and Applied Genetics*, vol. 123, no. 7, pp. 1075–1088, 2011.

[5] M. Zeleke, M. Adem, M. Aynalem, and H. Mossie, "Cotton production and marketing trend in Ethiopia: a review," *Cogent Food & Agriculture*, vol. 5, no. 1, article 1691812, 2019.

[6] S. Kumar, A. Jain, A. P. Shukla et al., "A comparative analysis of machine learning algorithms for detection of organic and nonorganic cotton diseases," *Mathematical Problems in Engineering*, vol. 2021, 18 pages, 2021.

[7] J. Farooq, A. Farooq, M. Riaz et al., "Cotton leaf curl virus disease a principle cause of decline in cotton productivity in Pakistan (a mini review)," *Canadian Journal of Plant Protection*, vol. 2, pp. 9–16, 2014.

[8] M. N. Sattar, A. Kvarnheden, M. Saeed, and R. W. Briddon, "Cotton leaf curl disease–an emerging threat to cotton production worldwide," *Journal of General Virology*, vol. 94, no. 4, pp. 695–710, 2013.

[9] R. W. Briddon, "Cotton leaf curl disease, a multicomponent begomovirus complex," *Molecular Plant Pathology*, vol. 4, no. 6, pp. 427–434, 2003.

[10] A. Fouda, A. El-Hadidy, and A. El-Deeb, "Mathematical modeling to predict the geometrical and physical properties of bleached cotton plain single jersey knitted fabrics," *Journal of Textiles*, vol. 2015, Article ID 847490, 10 pages, 2015.

[11] R. Levins and I. Miranda, "Mathematical models in crop protection," *Revista de Protección Vegetal*, vol. 22, no. 1, pp. 1–17, 2007.

[12] G. Hernández-Bautista, I. A. García-Montalvo, A. D. Pérez-Santiago et al., "Numerical simulation of dyeing process of cotton with natural dye," *PRO*, vol. 9, no. 12, p. 2162, 2021.

[13] H. Banks, J. Banks, J. Rosenheim, and K. Tillman, "Modelling populations of Lygus hesperus on cotton fields in the San Joaquin valley of California: the importance of statistical and mathematical model choice," *Journal of Biological Dynamics*, vol. 11, supplement 1, pp. 25–39, 2017.

[14] A. Mamatov, A. Parpiev, and M. Shorakhmedova, "Mathematical model for calculating the temperature field of a direct-ow drying drum," in *Journal of Physics: Conference Series*, vol. 2131, IOP Publishing, 2021.

[15] B. Dome, D. Kuznetsov, and Y. Nkansah-Gyekye, "A mathematical model that estimates input demand in respect to the costs for cotton production," *American Academic Scientific Research Journal for Engineering, Technology, and Sciences*, vol. 14, no. 1, pp. 187–203, 2015.

[16] M. Sundar Rajan and M. Palanivel, "Comparison of non-linear models to describe growth of cotton," *International Journal of Statistics and Applied Mathematics*, vol. 2, no. 4, pp. 86–93, 2017.

[17] A. Aboukarima, H. Elsoury, and M. Minyawi, "Simple mathematical models for predicting leaf area of cotton plant,"

Journal of Soil Sciences and Agricultural Engineering, vol. 6, no. 2, pp. 275–294, 2015.

[18] L. Su, Q. Wang, C. Wang, and Y. Shan, "Simulation models of leaf area index and yield for cotton grown with different soil conditioners," *PLoS One*, vol. 10, no. 11, article e0141835, 2015.

[19] J. Khan, Z. Bashir, A. Ahmad, W. Tariq, A. Yousaf, and M. Gohar, "Mathematical modeling of cotton leaf curl virus with respect to environmental factors," *European Journal of Microbiology and Immunology*, vol. 5, no. 2, pp. 172–176, 2015.

[20] A. Ahmad, N. A. Yasin, A. Ibrahim et al., "Modelling of cotton leaf curl viral infection in Pakistan and its correlation with meteorological factors up to 2015," *Climate and Development*, vol. 10, no. 6, pp. 520–525, 2018.

[21] F. Saeed, J. Farooq, A. Mahmood, M. Riaz, T. Hussain, and A. Majid, "Estimation of genetic variability for cotton leaf curl virus disease, fiber quality and some morphological traits using multivariate analysis in exotic gossypium (diploid and tetraploid) species," *Journal of Agrobiology*, vol. 30, no. 2, pp. 107–115, 2013.

[22] T. Kinene, L. S. Luboobi, B. Nannyonga, and G. G. Mwanga, *A mathematical model for the dynamics and cost effectiveness of the current controls of cassava brown streak disease in Uganda1*, UNCST, 2015.

[23] P. Van den Driessche and J. Watmough, "Reproduction numbers and sub-threshold endemic equilibria for compartmental models of disease transmission," *Mathematical Biosciences*, vol. 180, no. 1-2, pp. 29–48, 2002.

[24] C. Castillo-Chavez, S. Blower, P. Van den Driessche, D. Kirschner, and A.-A. Yakubu, *Mathematical Approaches for Emerging and Reemerging Infectious Diseases: Models, Methods, and Theory*, vol. 126, Springer Science & Business Media, 2002.

[25] A. K. Fantaye and Z. K. Birhanu, "Mathematical model and analysis of corruption dynamics with optimal control," *Journal of Applied Mathematics*, vol. 2022, Article ID 8073877, 16 pages, 2022.

[26] J. P. LaSalle, "Stability theory and invariance principles," in *Dynamical Systems*, pp. 211–222, Elsevier, 1976.

[27] H. S. Rodrigues, M. T. T. Monteiro, and D. F. Torres, "Sensitivity analysis in a dengue epidemiological model," *Conference Papers in Science*, vol. 2013, Article ID 721406, 7 pages, 2013.